J Solid State Electrochem (2001) 5: 119–130

ORIGINAL PAPER

A.V. Churikov · I.M. Gamayunova

Photoelectrochemical processes on metal electrodes in nonaqueous solutions of lithium salts

Received: 22 February 1999 / Accepted: 27 January 2000

Abstract The photoelectrochemical performance of lithium in a propylene carbonate solution of $LiClO_4$ and in a mixture of propylene carbonate with dimethoxyethane, as well as in a $LiAlCl_4$ solution in thionyl chloride, has been investigated. It has been established that when illuminating the electrodes under study, electronic photoemission takes place from the metal into a passivating film permanently existing on the lithium surface. The measurements were in part carried out with the Li electrode coated specially with a Li_2O or Li_2CO_3 protecting film. Photoemission spectroscopy has been used as a tool for exploring the processes of both formation and change in the composition and properties of the passivating layers on the lithium electrodes. The results for the photoelectrochemistry of lithium have been compared with the analogous data obtained with electrodes made of gold and SnCd alloy in a propylene carbonate solution of $LiClO_4$. In the two last cases, electronic photoemission from the metal into solution has been revealed.

Key words Lithium batteries · Lithium electrode · Passivating films · Photoelectrochemistry · Photoemission

Introduction

It is known that the application of lithium as the anode in lithium batteries is feasible owing to its high stability in contact with nonaqueous electrolyte solutions [1]. The stability is provided by the spontaneous formation, on the electrode surface, of a solid passivating film (PF) possessing the properties of a solid electrolyte, namely a relatively high ionic conductivity and poor electronic conductivity [1–3]. The passivating film on lithium is a thin continuous layer of insoluble products of metal interaction with the solution components, that comprises a dense part in the vicinity of the metal and a porous part exposed to the solution. The electrochemical behaviour of a Li electrode is determined mainly by the PF dense component, the thickness of which depends on the type of electrolyte system used and on the conditions of electrode storage in solution.

The composition and properties of passivating films on lithium have been extensively studied by means of different electrochemical and physicochemical methods [1–18]. One of the methods providing much information on the structure and properties of a metal/electrolyte solution interface is the photoelectrochemical method [19]. The use of the latter makes it possible, among other applications, to investigate the metal's behaviour in a passivated state [20]. This is why it would be of interest to apply the photoelectrochemical method to research into the processes of formation and change in the properties of passivating layers on Li.

For metals coated with passivating films, in general, different photoeffects are possible and, correspondingly, different functional dependences of the quantum yield η (or photocurrent I_{ph} proportional to it) on the potential E and on the energy of absorbed light quantum $h\nu$ could be observed. An internal photoeffect in the film takes place provided that the passivating film absorbs a light quantum with energy sufficient for electron excitation into a conduction band. The photocurrent caused by generating the electron-hole pairs in the PF is proportional, in the case of interest to us as thin films and poor absorption (edge of own absorption of a solid), to the linear coefficient of absorption α [19, 20]. For crystalline materials the following dependence of α on $h\nu$ takes place:

$$\alpha = K\frac{(h\nu - E_g)^n}{h\nu} \quad (1)$$

where K is a multiplier, E_g is the band gap width of a solid, and $n = 1/2$ for direct transitions and $n = 2$ for

A.V. Churikov (✉) · I.M. Gamayunova
Department of Chemistry, Saratov State University,
Astrakhanskaya str. 83, 410026 Saratov, Russia
e-mail: churikovav@info.sgu.ru
Tel.: +7-8452-516413; Fax: +7-8452-721491

indirect transitions. However, on frequent occasions, especially for amorphous materials, the dependence of the absorption coefficient on the quantum energy cannot be approximated by a power function, but obeys the empirical Urbach rule [20, 21]:

$$\alpha = \alpha_0 \exp\left(\gamma \frac{h\nu - E_g}{kT}\right) \tag{2}$$

where k is the Boltzmann constant, T is the absolute temperature, and γ is a constant dependent on the system's properties, in particular, on the structure perfection of a solid [22] (for films, $\gamma < 1$). There are also different interrelations between the photocurrent and the electrode potential, typical ones being the following:

$$I_{ph} \propto (E - E_{fb})^{1/2} \tag{3}$$

and

$$I_{ph} \propto \exp\left(\frac{\beta F^{1/2}}{rkT}\right) \tag{4}$$

Here E_{fb} is the flat-band potential, F is the electric field strength in the film, $\beta = (e^3/\pi\varepsilon\varepsilon_0)^{1/2}$, e is the elementary charge, $\varepsilon\varepsilon_0$ is high-frequency dielectric constant, and r is equal to 1 or 2. Equation 3 shows the characteristic potential dependence of the space-charge region thickness, in which electron-hole pair separation occurs, and Eq. 4 reflects the field dependence of the photocurrent due to the Poole-Frenkel effect on the presence of a high number of localized states in the band gap [19, 20].

Provided that incident radiation is absorbed by the metal, the photoemission of electrons or holes from the metal into the PF or through the PF directly into solution is possible. In the first case, the spectral characteristic near the absorption edge is described by the Fowler law for photoemission from a metal into a dielectric [23, 24]:

$$\eta = K(h\nu - w)^2 \tag{5}$$

where w is work function for an electron or hole from the metal into the film (red edge of the photoeffect). In the case of photoemission into a concentrated electrolyte solution, the photoemission process is described near the threshold by the 5/2 power law [23, 25]:

$$\eta = K(h\nu - w(0) - eE)^{5/2} \tag{6}$$

where $w(0)$ is the electronic work function of the metal into the solution at $E = 0$. There are indications that in a more general case the dependence of the photoemission quantum yield on E and $h\nu$ is described by the power law:

$$\eta = K(h\nu - w(0) - eE)^n \tag{7}$$

with an exponent of a power $n > 2$ dependent on the parameters of a potential barrier for emitted electrons formed by a double electric layer [26, 27]. In particular, the n values are higher with the greater height and thickness of the potential barrier, which has been confirmed experimentally (n values from 2.45 to 3.35 were obtained) [26–28]. As follows from Eqs. 6 and 7, the additivity should take place between the quantities of the electronic work function $w(E)$ and the electrode potentials E at which these w have been deduced:

$$w(E) = w(0) + eE \tag{8}$$

If the photoemission into a diluted electrolyte solution occurs, it is described by the so-called modified 5/2 power law, taking into account a potential drop in the space-charge region [25]:

$$\eta = K(h\nu - w(0) - e(E - \psi'))^{5/2} \tag{9}$$

where ψ' is the potential drop across the diffuse part of the double electric layer. In any case, Eqs. 5–9 allow one to identify photoemission due to the characteristic form of the absorption edge and the characteristic dependence on the electrode potential, as well as the additivity between w and E on photoemission into solution [20].

In our previous work [29] concerned with the photoelectrochemistry of a lithium electrode exposed to nonaqueous electrolyte solutions, it was shown that on pulse illumination of the electrode by light with $h\nu > 1$ eV, a fast cathodic photoeffect was observed. On the basis of studying the spectral and kinetic characteristics of the cathodic photoeffect, we have concluded that its primary step is electronic photoemission from metallic lithium into the PF [29–31]. For several electrolyte systems the values of the photoelectric work functions w were determined for electrons from Li into the film [29]. In the present work the problem of the photoprocess nature of Li in nonaqueous solutions is also discussed, and it is proposed to determine the PF compositions formed on Li in several electrolytes, by measurements of the electronic work functions and comparisons of the obtained w values with the data for model systems with defined compositions of PFs artificially formed on a lithium surface.

It seems reasonable to compare the photoelectrochemical data obtained for the Li electrode with the results of analogous experiments performed for other metals. Thus additional information and additional arguments can be extracted when solving the problem of the nature of the photoprocess on Li. Such a comparison is also undertaken in the present paper. We have chosen alloys of the system Li-Sn-Cd that is used as the anode in lithium accumulators [32, 33], as well as gold. A 1 M $LiClO_4$ solution in propylene carbonate (PC) served as the electrolyte, since the electrochemical behaviour of these metals in PC is rather well studied [34–39]. The choice of such electrodes is based on the fact that the surfaces of the initial Au, Sn, Cd metals and SnCd alloy do not react with the electrolyte, and photoelectrochemical behaviour different from that of Li could be expected. However, at a low potential and with cathodic intercalation of lithium in the electrodes, a passivating film forms on the latter analogous to the PF on pure Li and similar in chemical composition [35–39]. One could therefore follow the effect of lithium intercalation and passivating film formation upon the photoprocess characteristics exemplified by these electrodes.

Experimental

The measurements were conducted in three-electrode hermetically sealed cells with an optical quartz window, which were assembled in a glove box in an atmosphere of dry argon. The counter electrode and reference electrode were made from lithium. The lithium working electrode was made by pressing metallic Li in a glass tube. Exposed to a solution was the electrode face, produced by cutting out excess lithium, and having a surface area of 0.04 cm^2. In addition, the measurements were carried out in part with the Li electrodes coated with oxide (Li_2O) or carbonate (Li_2CO_3) film formed beforehand and obtained by annealing the lithium electrodes at 370 K or 380 K in an atmosphere of dry pure O_2 or dry pure CO_2, respectively.

The Au electrode was made from gold foil, boiled in concentrated HNO_3, washed, and dried. The SnCd electrode was formed by coating the melt on a Ni support. We used electrodes containing 20 mol% Cd. The working surface area of the electrodes was 0.15 cm^2; a non-illuminated surface was isolated. For determining the perfect polarizability region of the Au and SnCd electrodes, cyclic voltammograms were obtained in advance using a PI-50-1 potentiostat with a PDA1 registering device.

Along with a 1 M $LiClO_4$ solution in PC, a 1 M $LiClO_4$ solution in a mixture of PC with dimethoxyethane (DME) in a ratio of 7:3 and a 1 M $LiAlCl_4$ solution in thionyl chloride (TC) were used in the present work. The water content in the organic solutions was 50 ppm. Furthermore, special measurements were performed in 1 M $LiClO_4$ in PC + DME solution at a moisture content of 1000 ppm. Photoelectrochemical measurements and the cells' storage under open-circuit conditions took place at 298 K. In the course of the storage, the thickness and specific ionic conductivity of the PF were controlled using impedance and voltammetric measurements, as described earlier [39–42].

The potential dependences of the photocurrent were registered using a potentiostat. On spectral photo measurements, the working electrode potential was obtained by means of a battery with a divider. As is accepted for lithium electrochemical systems, all the potentials in this paper have been presented in respect to the Li/Li^+ electrode in the same solution. In the course of measurements the working electrode was illuminated through a solution layer (the solutions applied here do not absorb visible, near-UV, or IR light; appreciable absorption by the PC solution was observed at wavelengths less than 250 nm, and by the TC solution at less than 350 nm [43]). We used the pulse technique for the photoelectrochemical measurements. The pulse supply of monochromatic light with a pulse duration of 0.1 ms at half-height consisted of a pulse xenon lamp with a power supply, condenser system, and monochromator. A signal appearing from a single light pulse was registered using a S8-13 memory oscillograph and recalculated into the quantum yield η in terms of the incident light. The photons incident flow was determined using certified photoelements. For the spectral band involved here (400–1000 nm), it ranged from 5×10^{16} to 5×10^{17} s^{-1} cm^{-2}.

Results and discussion

Nature of the photoeffect on the Li electrode

At all potentials, the lithium electrode behaves reversibly; thus there is a problem of registering the potential dependence of the photocurrent within a wide range without changes in the state of the electrode surface. Therefore we obtained the dependences of I_{ph} versus E at small variations of the Li potential relative to the equilibrium one, the electrode being polarized for short periods (at the moment of measurement) in order to avoid a prominent change in the PF. An analogous technique was applied also for registering the spectral dependences of the photocurrent, which were measured either at the Li equilibrium potential or at slight potential deviations from the equilibrium one. In all the cases studied, when illuminating the lithium electrode by monochromatic light with the appropriate wavelength, only one cathodic photocurrent was observed. The photoresponse was fast, i.e. the form of the current response coincided almost entirely with the form of the light pulse, as Fig. 1 shows. Figure 1 also provides information on the order of the values of the photocurrent measured. Altogether, several million unit measurements were carried out, and several hundred spectra registered; only one cathodic photoprocess was observed in all the measurements (we ignore here a false signal that appeared owing to electrode heating and manifested itself at great deviations of potential from the equilibrium one as a dark current modulation; this point is discussed in [29, 43]).

Figure 2 shows the dependences of the quantum yield on the potential for the Li electrode in the 1 M $LiClO_4$ in PC + DME solution. These dependences are linearized satisfactorily for $\eta^{1/n}$ versus E at $n = 2$ or $n = 2.5$, which correspond to Eqs. 5 and 6 for the applicability of photoemission from the metal. Attempts to determine more precisely the power exponent from the η versus E dependences fared poorly. However, what was established absolutely reliably is that for describing the experimental η versus E dependences of the Li electrode, Eqs. 3 and 4 are not applicable at all for the internal photoeffect.

Thus, on illumination of the lithium electrode, the internal photoeffect in a PF does not occur, and the cathodic photocurrent observed is obviously caused by photoemission. The sign of the photocurrent points to electronic photoemission. The same conclusion was made by us earlier [29]. A PF on Li is a thin (about 10 nm) transparent formation composed of lithium salts

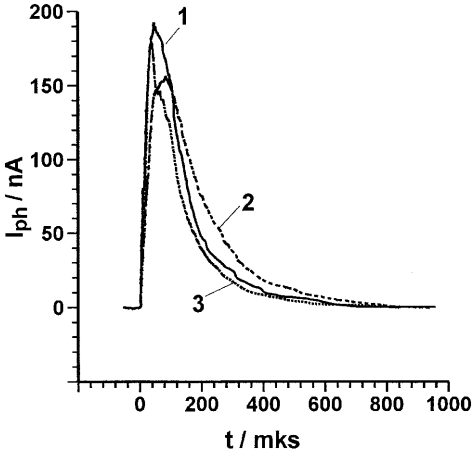

Fig. 1 Photoresponse of the Li electrode freshly prepared (*1*) and after 1-week storage in the electrolyte (*2*) in response to the light pulse (*3*). Electrolyte is 1 M $LiClO_4$ in PC + DME; $\lambda = 550$ nm

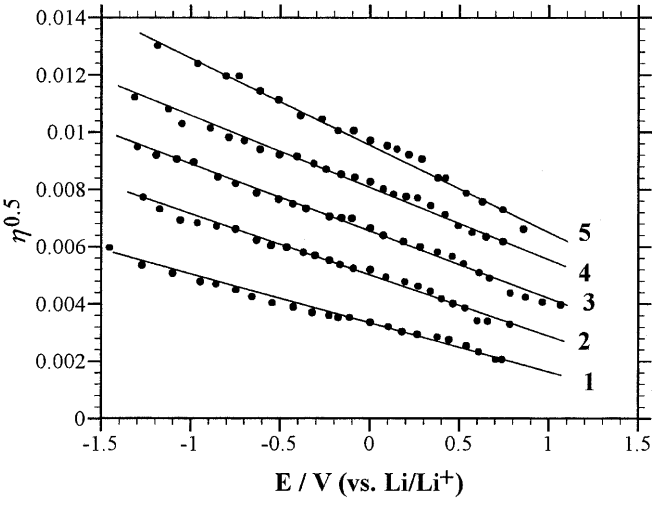

Fig. 2 Potential dependences of the photocurrent on the Li electrode in 1 M $LiClO_4$ in PC + DME at quantum energies (eV) of 1.530 (*1*); 1.771 (*2*); 2.000 (*3*); 2.398 (*4*); 2.883 (*5*). Duration of electrode storage in solution is 3 months

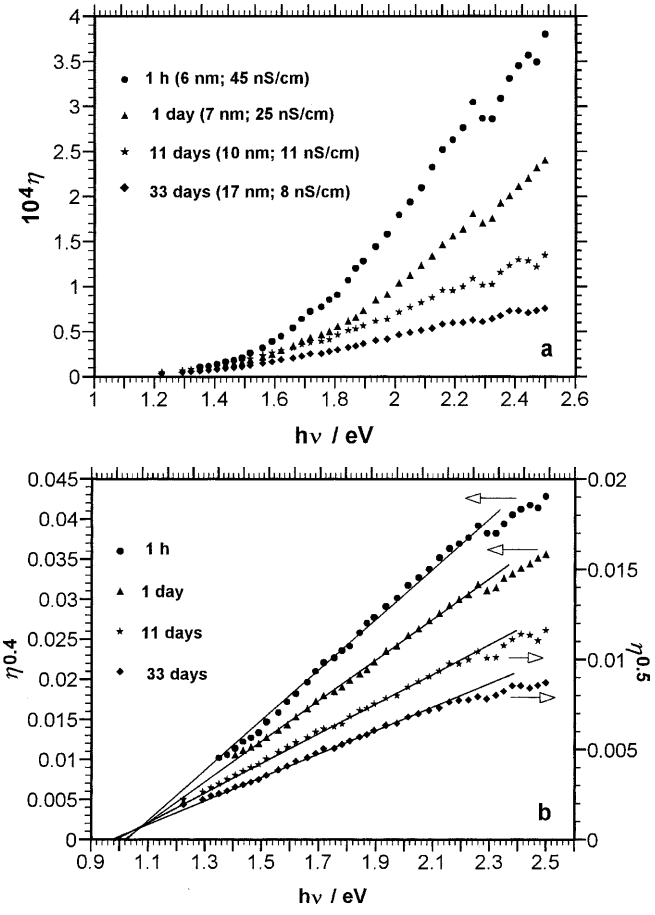

Fig. 3a, b Spectral dependences of the photocurrent on the Li electrode in 1 M $LiClO_4$ in PC + DME presented for different variables. Duration of electrode storage in solution, PF thickness, and its electroconductivity are indicated in figure

(Li_2O, Li_2CO_3, LiCl, LiF, lithium alkoxides and alkylcarbonates [4–16, 34–38]), which are substances with wide band gaps not absorbing visible light. This is why the internal photoeffect seems unlikely to occur.

Figure 3a depicts the typical spectral characteristics of the cathodic photocurrent at $E = 0$ for the Li electrode in a solution of 1 M $LiClO_4$ in PC + DME. The spectra were recorded during the course of cell storage accompanied by growth in the PF thickness and its aging [1–3, 8, 16, 39–42] (the corresponding values of the PF thickness and electroconductivity are mentioned on the figure). Very similar spectral dependences for the photocurrent were obtained in all the lithium electrochemical systems in our study. These are superlinearly increasing curves, the slope of which declines slightly during the electrode aging. For describing such curves, both the photoemission of Eqs. 5–7 and Eq. 1 at $n = 2$ are applicable, provided that the internal photoeffect in the film is assumed. The most adequate description is achieved with Eqs. 5 and 6, worse with Eq. 1. In general, this confirms the conclusion made above on the photoemission nature of the photoeffect on the Li electrode.

Thus, on lithium electrode illumination, light is not absorbed by the passivating layer but reaches the metal surface, causing the photoemission. Such an interpretation of the nature of the photoprocess on lithium does not conflict with the observed values of the quantum yield (10^{-5}–10^{-3}) typical for photoemission [19]. It is indirectly supported also by a photoprocess kinetics study [30]. The time dependences of the photocurrent and photopotential after electrode illumination by the laser nanosecond pulse are simulated well by the equations, involving fast electronic emission from the metal with their consequent delayed diffusion in the medium.

We examined earlier [29] the power law validity for describing the I_{ph} versus $h\nu$ spectra of lithium by means of the method of photocurrent logarithmic derivatives consisting of differentiation of the experimental log I_{ph} versus $h\nu$ or logI_{ph} versus E curves, which allows one to find simultaneously both n and $w(0)$ [26–28]. This method requires highly precise measurements. As a result, we [29] previously determined the values of the work function $w(0) \approx 1$ eV and exponent n close to 2.5 for the freshly prepared electrodes, with n values somewhat declining (down to $n \approx 2$) in the course of cell storage. These quantities in general have found their confirmation also in the present work. Table 1 shows the results of computational treatment of the typical series of experimental η versus $h\nu$ curves according to Eq. 7 in logarithmic form; thereupon n and $w(0)$ served as adjustment parameters calculated from a condition of minimal variance between the experimental and calculated curves. A somewhat declining value of n at unchanged $w(0) \approx 1.0$ eV was commonly observed in the course of cell storage. Although different intermediate n values could be obtained on this way, we will hereafter prefer Eqs. 5 and 6 as the most substantiated theoretically. Thus we will approximate n by 2 or by 5/2 and present the experimental spectra in the plots of $\eta^{0.5}$

Table 1 The results of computed processing of a typical series of Li electrode spectra using the equation $\log \eta = \log K + n\log(h\nu - w(0))$. The electrolyte is 1 M $LiClO_4$ in PC + DME

Cell age (days)	n	$w(0)$ (eV)
0.1	2.86	0.97
1	2.93	0.96
4	2.94	0.96
6	3.02	0.94
11	2.74	1.00
15	2.23	0.95
30	2.06	0.96
60	2.01	0.96

versus $h\nu$ or $\eta^{0.4}$ versus $h\nu$ as corresponding to Eqs. 5 and 6 linearization. As is seen from Fig. 3b, fairly straight lines are achieved in these plots.

The part of the medium into which the electronic emission occurs can also be elucidated on the basis of studying the spectra. The Fowler law (Eq. 5) validity, which is in general true for photoemission from a metal into a vacuum or a dielectric [23–25], means that in our case, too, the photoemission into a poorly conducting medium takes place. In this connection one could believe that the terminal state of the emitted electrons is in the passivating film. Figure 4 depicts the series of η versus $h\nu$ spectra registered in the 1 M $LiClO_4$ in PC solution at slight variations of the Li electrode potential. The same spectral curves as in the PC + DME solution (Fig. 3b) are obtained in the PC solution. Along with the above-mentioned decrease in the exponent of the power during electrode storage, as is seen from Fig. 4, the additivity between a shift of the photoeffect red edge Δw and change in the electrode potential ΔE (Eq. 8), peculiar for photoemission into an electrolyte, was not observed. Finally, as will be demonstrated below by measurements with other metals, the value of the electronic work function directly into the PC solution is different.

The data obtained could be explained by the following. Li is characterized by the electronic photoemission into the surface PF described by the Fowler law in the case of poor electroconductivity of the PF. The straight lines observed from Fig. 4c correspond to Eq. 5. However, the freshly formed PFs have been established to possess an increased concentration of mobile ionic defects (up to 10^{-2} M) [39–42]. In this case the photoemission into the PF must be described in the same manner as photoemission into the dilute electrolyte solution, namely by Eq. 9. The spectral dependences of the photocurrent are linearized in the plots of $\eta^{0.4}$ versus $h\nu$, but there is no additivity between $w(E)$ and E, since ΔE is partially ascribed to the interface and another part of ΔE drops across the bulk of the film (space charge region in the film). In the PF during storage, contemporary to its growth, the relaxation processes also occur leading to the change in the PF conducting properties (recrystallization of the film, disappearance of the defects). The most rapid relaxation takes place during the first hours after PF formation [41, 42]. This results in diminution of the PF specific ionic electroconductivity (see Figs. 3, 4). The calculations show that for several weeks of Li electrode storage in the PC solution, the concentration of the mobile ionic defects in the PF decreases from 10^{-2}–10^{-3} M to 10^{-3}–10^{-4} M, and in the TC solution to $\sim 10^{-5}$ M [41, 42]. This could be a reason for going from the spectral 5/2 power law (Eq. 9) to the square law (Eq. 5). The work function remains unchanged and equals $w(0) = 1.0 \pm 0.05$ eV for the films formed in the PC solution. Figure 4 also shows that the threshold energy w value alters on change in the Li electrode potential. The longer is the duration of the electrode storage in solution, the lesser pronounced is the effect of E on w. This can be explained by the decrease in the voltage portion applied to the Li|PF interface due to the PF thickness growth and its electroconductivity diminution with time.

In closing the section let us discuss the evolution with time of the photosensitivity of the Li electrode exposed to the electrolyte aprotic solution. The photosensitivity criterion could be a value of the quantum yield at a certain wavelength or the value of the multiplier K in Eqs. 5, 6, 7 at a given n and w. Figure 5 shows η quantities at a quantum energy of 2.25 eV corresponding to the validity of the power spectral law (Fig. 3). There are presented also the values of the photogenerator internal resistance R_i determined by a decrease in the Li electrode photopotential on connecting the cell to an external load. A decline of the photosensitivity was commonly observed in the course of cell storage. Sometimes more complicated behaviour took place, namely a photosensitivity increase during the initial period was followed by a further dramatic decrease. As for the photopotential measured under the open circuit conditions, initially its growth was always observed followed by the stabilization or diminution. From the viewpoint of photoemission into the PF, the value of the photocurrent into an external circuit depends on the film thickness, the electron emission length, the electron diffusion coefficient, and the strength and direction of the internal electric field in the PF; the theory of the

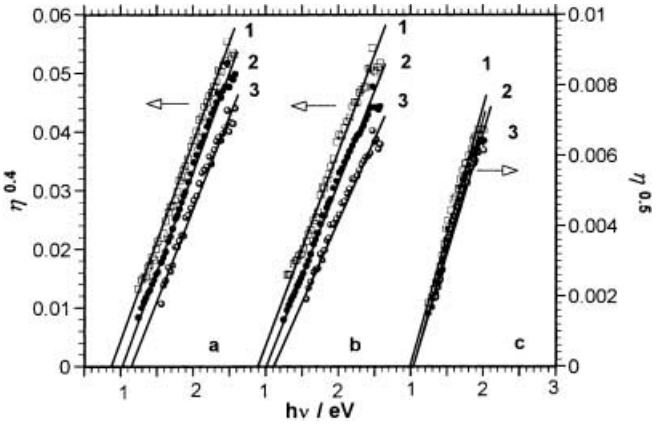

Fig. 4a–c Spectral dependences of the photocurrent with the Li electrode in 1 M $LiClO_4$ in PC at a potential (V, relative to Li/Li^+) of −0.2 (*1*); 0.0 (*2*); 0.2 (*3*). Storage duration: **a** 3 h; **b** 3 days; **c** 100 days

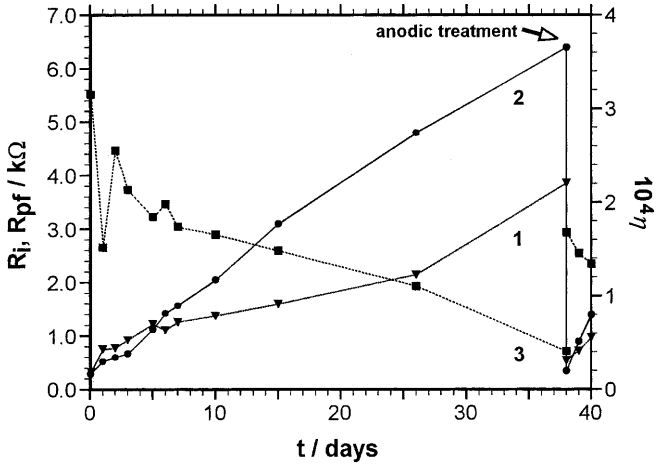

Fig. 5 Evolution with time for photogenerator internal resistance R_i (*1*), film resistance R_{PF} (*2*), and quantum yield at $\lambda = 550$ nm on the Li electrode in 1 M $LiClO_4$ in PC (*3*)

phenomenon can be found elsewhere [30, 44]. The gain in PF thickness occurring continuously with time must lead to the decrease in the photoemission quantum yield, that we indeed observed in the experiment. However, provided that other parameters also change at the same time, the result can be a complicated behaviour of the photosensitivity with time. As for the photopotential, the gain in photogenerator internal resistance R_i with time is of decisive importance. Resistance R_i and the ionic resistance of the passivating film R_{PF} are close to each other and change with time in a similar manner, although not coinciding (Fig. 5). Obviously the increase in both resistances just mentioned is due to the growth of the PF thickness and the diminution of the PF electroconductivity during storage. Li electrode treatment by passing an anodic current, resulting in PF destruction and a sharp decrease of R_i and R_{PF}, also resulted in a gain of the photosensitivity, which finds a natural explanation within the framework of the above performances.

Photoemission and composition of passivating films on lithium

A large number of investigations are concerned with exploring the chemical composition of PFs on lithium (see, e.g., [4–16]). It would be of interest to use the photoemission measurements for determining the composition of PFs on Li. Since the photoemission energy characteristics depend on the composition of the medium in which an emitted electron occurs, there is an opportunity for estimating the PF chemical composition by means of photoemission spectroscopy, comparing the values of the electronic work function of Li into an unknown film with those values for a film of identified chemical composition. Such data are partly presented in [29]. The case in point there is the composition of a layer in the vicinity of the metal surface, the thickness of which corresponds to a photoemitted electron path.

The compositions of the PFs forming on Li in many solvents and electrolyte solutions used in lithium power sources have been extensively studied [4–18]. PFs formed on Li in PC solutions seem to have been investigated most thoroughly [5–14]. Thus, in the series of papers by Kanamura et al. [5–7] it has been shown that the initial "native" PF on Li is non-uniform in composition: an internal thin layer of Li_2O is coated by external thick layer of Li_2CO_3 and LiOH. Similar data have been obtained by others [4, 15]. According to some [7], such a composition and structure of the PF remain principally the same even after submerging lithium in the PC solution. A dense part of the PF in the vicinity of the electrode is due to reaction with traces of water and consists of Li_2O, whereas a porous part of the PF exposed to the solution can include other compounds [8]. This was confirmed in the series of papers by Aurbach et al. [9, 10, 11], where the primary products of Li reaction with PC were shown to be lithium alkylcarbonates capable of further interacting with traces of water in solution, yielding Li_2CO_3. Li_2O contact with PC results in alkylcarbonate formation also, so Li_2O could be contained only in an internal part of the PF, and the stable final product of the PF chemical transformation is Li_2CO_3. In the case of mixed solvents, e.g. PC + DME, the film consists of lithium alkoxides and alkylcarbonates, yielding Li_2CO_3 in the presence of traces of water [10]. On the other hand, Nazri and Muller [14] believe that, in contrast, the PF in anhydrous solutions consists of hydrocarbon polymers and Li_2CO_3, and the gain in moisture content in solution leads to their replacement with Li_2O.

In Fig. 6a–d are depicted the spectral dependences of electronic photoemission from Li into PFs measured in 1 M $LiClO_4$ in PC + DME at the equilibrium potential of the Li/Li^+ electrode. The electrodes vary in the methods of their surface preparation: in a and d, by cutting under the solution layer; in b, by annealing in an atmosphere of O_2, yielding Li_2O; in c, by annealing in an atmosphere of CO_2, yielding a Li_2CO_3 layer. In addition, in cases a and d the solution contained 1000 ppm of water. For the freshly formed PF, the spectra are straight lines for $\eta^{0.4}$ versus $h\nu$, commonly converting into the $\eta^{0.5}$ versus $h\nu$ straight lines on electrode aging. The reason for this transformation has been already discussed above. The work function $w(0)$ for the systems presented in Fig. 6 does not change with time. This means the conservation of the PF chemical composition in the course of Li electrode storage in solution, at least through a distance corresponding to the final state of the emitted electrons, i.e. in an internal PF region.

A PF composition could be determined by comparing the $w(0)$ values for the PFs obtained spontaneously and artificially. For the Li electrode formed in the PC or PC + DME solutions, the work function $w(0) = 1.0 \pm 0.05$ eV in an anhydrous solution and 0.8 ± 0.05 eV in a moist solution (Figs. 3, 4, 6a). For the Li electrode annealed in a gaseous atmosphere, the work function was 1.0 ± 0.05 eV for the oxide PF and 0.8 ± 0.05 eV

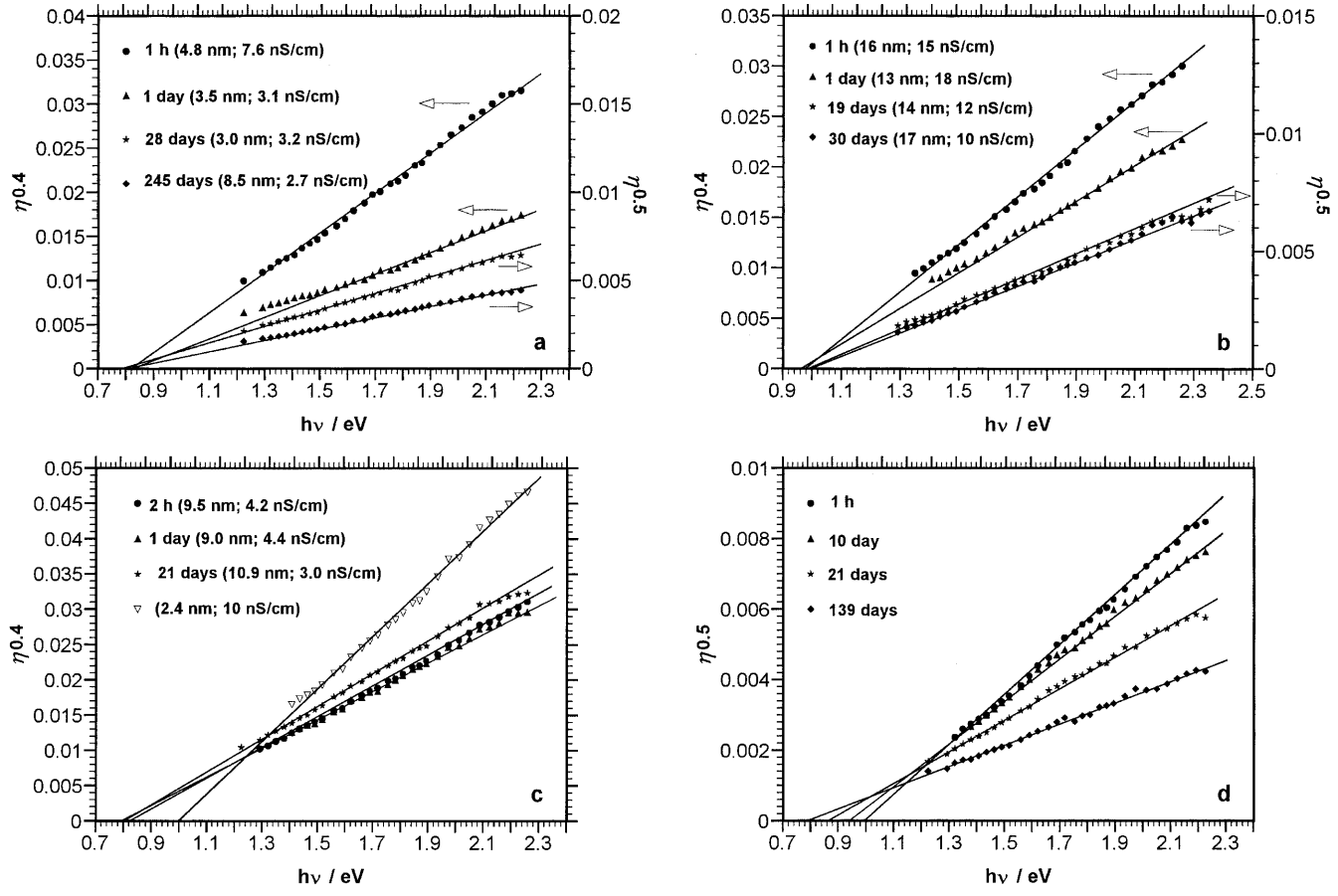

Fig. 6a–d Spectral dependences of the photocurrent with the Li electrode in 1 M $LiClO_4$ in PC + DME. **a**, **d** Electrode surface cut off in electrolyte; **b** electrode surface annealed in oxygen; **c** electrode surface annealed in CO_2 (curve ∇ after cutting off electrode surface in electrolyte); **a** solution contains 1000 ppm H_2O; **d** electrode is transfered from dry solution (after 60 days of storage) into solution with 1000 ppm water content. Storage duration, PF thickness, and its electroconductivity are indicated on the figure

for the carbonate PF (Fig. 6b, c). From the above reasoning one can conclude that the PF on Li in sufficiently dry PC and PC + DME solutions consists of Li_2O, in agreement with other data [6–11]. In the PC and PC + DME solutions at the increased water content, the film consists of Li_2CO_3, which is also in conformity with other results [9–11]. In support of this conclusion is the rather indicative experiment involving carbonate layer removal by means of cutting off the electrode surface under the solution layer, immediately leading to a sharp increase in $w(0)$ from 0.8 to 1.0 eV (Fig. 6c).

Of interest is the point whether or not the change in the PF chemical composition takes place on substitution of the electrolyte solution. By means of measurements of the photocurrent spectral dependences one could follow, in a number of cases, the PF composition alterations. Figure 6d shows the evolution of the photoemission spectra as a result of the replacement of the anhydrous electrolyte by an electrolyte with a high water content. This caused $w(0)$ to diminish gradually from 1.0 to 0.8 eV, obviously because a carbonate film has taken the place of an oxide film. We will consider another instance of the change in PF chemical composition using the TC solution, in which the PF forms mainly from LiCl, as is conventionally believed [1, 18]. Figure 7a depicts the the spectral dependences of the electronic photoemission from Li cut off in 1 M $LiAlCl_4$ in TC into the film, measured at the electrode equilibrium potential. As in the case of the organic solution, the straight lines of $\eta^{0.4}$ versus $h\nu$ are observed for the freshly formed PF, transferring into the $\eta^{0.5}$ versus $h\nu$ straight lines on the gain in storage duration. The work function remained constant and equal to 1.3 ± 0.05 eV, being indicative of the constancy of the PF chemical composition when the system ages. However, alteration of the photoemission spectra is observed in the TC solution during storage of the Li electrode with an oxide film formed on its surface (Fig. 7b). Initially the spectral dependence was a $\eta^{0.4}$ versus $h\nu$ straight line with a threshold energy of 1.0 eV. The electrode storage in the TC solution was accompanied not only by a spectral law change, but also by a gradual increase in $w(0)$ from 1.0 to 1.3 eV. The value of $w(0) = 1.0$ eV is assigned, as is established, to electronic photoemission from Li into Li_2O, and the value of $w(0) = 1.3$ eV for Li into LiCl (Fig. 7a). Therefore, in this system, too, the photoelectrochemical method allows one to follow the replacement of the oxide film by a chloride one. Both cases exhibit the change in the PF

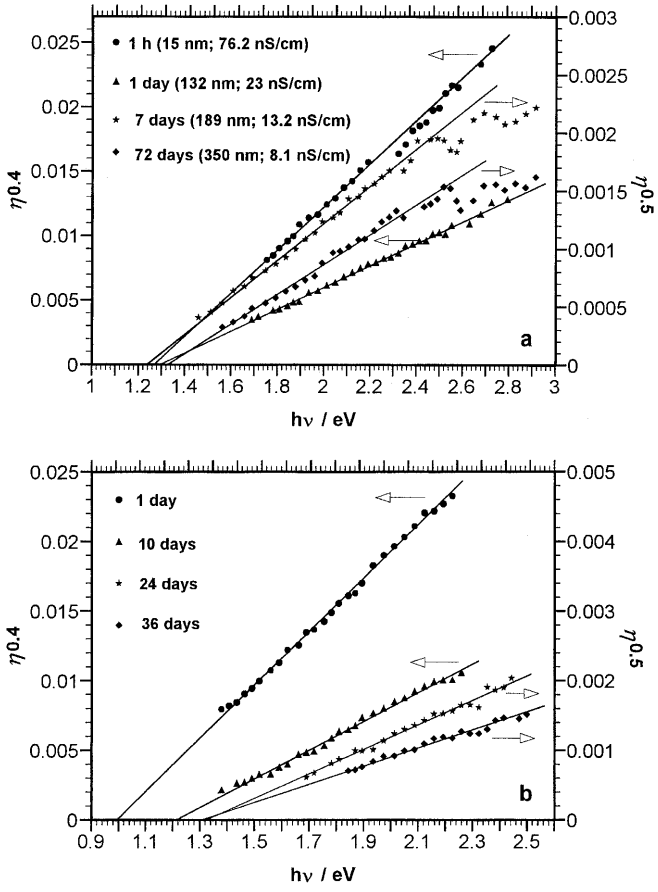

Fig. 7a, b Spectral dependences of the photocurrent with the Li electrode in 1 M $LiAlCl_4$ in TC. **a** Electrode surface is cut off in electrolyte; **b** electrode surface is annealed in oxygen. Storage duration, PF thickness, and its electroconductivity are indicated on the figure

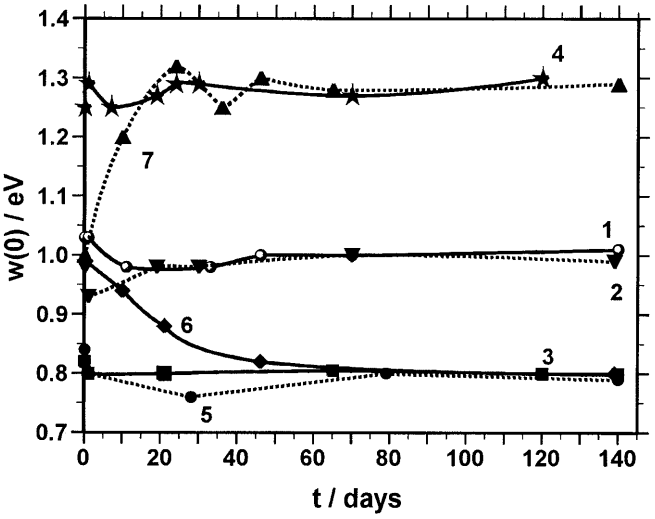

Fig. 8 Change in work function $w(0)$ with time in the systems Li|1 M $LiClO_4$ in PC + DME (*1*); Li|Li_2O|1 M $LiClO_4$ in PC + DME (*2*); Li|Li_2CO_3|1 M $LiClO_4$ in PC + DME (*3*); Li|1 M $LiAlCl_4$ in TC (*4*); Li|1 M $LiClO_4$ in PC + DME + 0.1% H_2O (*5*, *6*); Li|L_2O|1 M $LiAlCl_4$ in TC (*7*). The curve *6* PF is formed in 1 M $LiClO_4$ in PC + DME

chemical composition occurring not rapidly but over prolonged periods. Figure 8 summarizes the data presented in this paper on work function quantities $w(0)$ from Li into passivating films formed under different conditions.

In closing this section, let us note that although photoemission in general is not recognized as a well-reproducible phenomenon, nevertheless the lithium electrode photoresponse is reproduced rather well for different techniques of surface preparation and types of electrolytes used. Therefore the results presented in this paper allow one to consider photoelectrochemical spectroscopy as a promising method for determining the chemical composition of passivating layers on Li. It is capable of providing valuable information on the state of the Li electrode in lithium batteries, especially in combination with other methods, e.g. electrochemical ones.

Photoemission from Au and SnCd electrodes

In order to substantiate the conclusion that the photoemission from Li occurs into the PF, but not into the electrolyte solution, determination of the work function of Li into the solvent is essential in general. Since it is not possible to separate lithium from a film even for a short period, we investigated several metals in the PC solution with the intent of revealing the photoemission into the solution. The results of studying the photoemission properties of gold and SnCd alloy are given below.

Let us define first the potential region useful for studying photoemission, i.e. the region of these metals with perfect polarizability. The electrochemical performance of gold in various nonaqueous solutions of lithium salts was investigated earlier [34–38]. Thus, it was shown that PC and solutions based on it begin to undergo oxidation on Au at $E > 4$ V, and reduction at about 1 V, by the Li/Li^+ electrode. At $E < 0.2$ V, cathodic intercalation of Li into Au starts with alloy formation, and in the potential range of 3.3–4.0 V the formation of a gold hydroxide takes place [36, 37]. Cadmium and SnCd alloy begin to undergo oxidation in a PC solution at $E \approx 2.7$ V, tin at $E \approx 2.9$ V, and microcurrents are observed in a rather wide potential range of 0.8 V up to 2.7 V [39]. Lithium comes into intercalation in Cd from a PC solution at $E \approx 0.7$ V, in Sn at $E \approx 0.75$ V, an active formation of Li alloys with Cd occurs at $E < 0.2$ V, and with Sn at $E < 0.4$ V [39]. The range of potentials between the anodic and cathodic processes could be expected to be satisfactory for observing photoemission.

In Fig. 9 the stabilized cyclic voltammograms of SnCd and Au electrodes are presented in the potential ranges 0.85–2.55 V and 0.5–3.1 V, respectively. As was shown in [45], in the first cycle, some bumps of the cathodic current (near 0.9–1.2 V, 1.5–1.8 V, and 2.1–

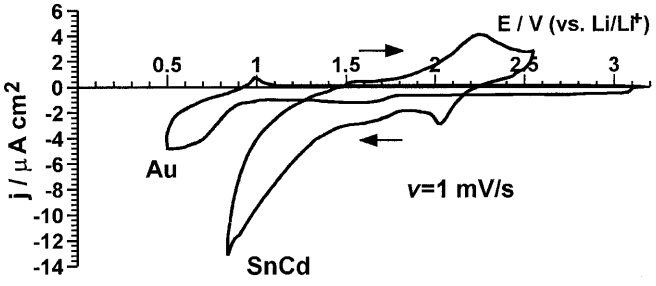

Fig. 9 Stabilized (10th cycle) cyclic voltammograms of Au and SnCd electrodes in 1 M $LiClO_4$ in PC. The scanning direction is shown by the *arrow*

2.3 V) appeared, not displayed in subsequent cycles. The analogous phenomenon observed with Au and Ag in different nonaqueous solutions was explained by reduction of microimpurities in the solution; a kink near 1.1 V was assigned to reduction of traces of water, and kinks near 2 V to oxygen reduction [35–37]. For the stabilized cyclic voltammograms, microcurrents are peculiar. In this potential region corresponding to the perfect polarization range for the electrode, its surface is apparently free of passivating layers. The increase in cathodic current for inert metals at the potentials more negative than 1 V is commonly related to the beginning of PC reduction that, in the presence of the Li^+ cation, leads to PF formation from insoluble carbonate and alkylcarbonates of lithium [37]. In general one can conclude that the range of potentials from the beginning of solvent reduction to the beginning of metal oxidation is appropriate for photostudies.

Figure 10 demonstrates, for $\eta^{0.4}$ versus E, the experimental dependences of the photocurrent upon the potential obtained at a constant quantum energy. Both for Au and SnCd electrodes on pulse illumination, one fast cathodic photocurrent similar to the Li electrode photoresponse was observed. In the region of sufficiently positive potentials, the $\eta^{0.4}$ versus E plots are straight lines with negative slopes, i.e. they obey Eq. 6. In the region of less positive potentials (at $E < 0.7$ V for Au and $E < 1.0$ V for the SnCd alloy), a drastic deviation from the 5/2 power law occurs. Returning to Fig. 9, one can conclude that the decrease in photocurrent observed is probably related to the beginning of the reduction of the solution components and to the consequent change in the electrode surface state. In spite of the distinct nature of the metals, the threshold potentials E_0 (intercepts on the E-axis) coincide within the experimental error ($E_0^{Au} = 1.86$ V and $E_0^{SnCd} = 1.87$ V). The characteristic dependence of photocurrent on the electrode potential and the independence of threshold potential on the metal-emitter nature means that, in both cases, just the electronic photoemission from the metallic electrode into the electrolyte solution is the primary step of the photoeffect, since in this situation the photoemission threshold should be determined only by the potential in accordance with Eq. 8 [25].

The spectral dependences of the photocurrent presented in Fig. 11 for $\eta^{0.4}$ versus $h\nu$ also obey Eq. 6. The choice of potential interval 0.91–1.21 V for measurements with inert electrodes is conditioned, on the one hand, by deviations from the $\eta^{0.4}$ versus E straight line in Fig. 10 at lower E values, and, on the other hand, by the sensitivity limit of the registering device, that does not allow a photoresponse to be measured at more positive potentials and low quantum energies. Figure 11 shows that additivity takes place between the quantities of the electronic work function $w(E)$ and electrode potentials E in accordance with Eq. 8. Indeed, for the spectral curves 2 and 3 measured with the SnCd electrode at distinct potentials, the electrode potential difference $\Delta E = 0.132$ V and the difference of the work functions $\Delta w = 0.12$ V; therefore, $\Delta w \approx \Delta E$. For the spectral curves 1 and 3 measured with different metals, $\Delta E = 0.30$ V and $\Delta w = 0.28$ V; thus, in this

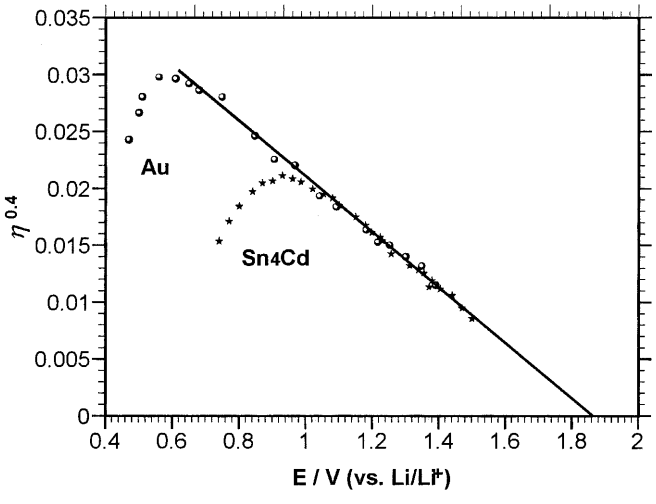

Fig. 10 Potential dependences of quantum yield with Au and SnCd electrodes in 1 M $LiClO_4$ in PC at quantum energy $h\nu = 2.552$ eV

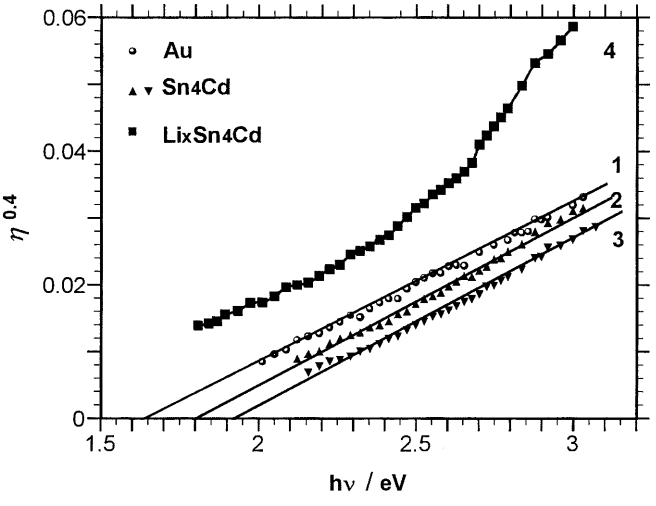

Fig. 11 Spectral dependences of quantum yield with Au, SnCd, and LiSnCd electrodes in 1 M $LiClO_4$ in PC. Electrode potential (V, relative to Li/Li^+): 0.910 (*1*); 1.078 (*2*); 1.210 (*3*); 0.475 (*4*)

case also $\Delta w \approx \Delta E$. At the same time, the spectral curve 4 obtained at the equilibrium potential of the SnCd electrode after its cathodic treatment (lithium intercalation from the solution) is not described by either the 5/2 power law or Eq. 7 at reasonable n values. More detailed discussion on the photoprocess nature concerning the LiSnCd electrode is presented at the end of this discussion.

No special electron acceptors were introduced into the solution, because the substances conventionally serving as acceptors (N_2O, or the ions H^+ or NO_3^- [19]) interact actively with lithium; their behaviour in non-aqueous media is also investigated insufficiently. Therefore, photoemission currents measured here are residual, i.e. related to electrons captured by the solution components.

Let us define the electronic work function of a metal into the PC solution $w(0)$ using Eqs. 6 or 8. This appears to be equal to 0.7 ± 0.05 eV (0.69 ± 0.03 eV and 0.70 ± 0.05 eV from the plots of $\eta^{0.4}$ versus E and 0.71 ± 0.03 eV and 0.71 ± 0.06 eV from the plots of $\eta^{0.4}$ versus $h\nu$ for Au and SnCd alloy, respectively). This quantity $w(0)$ differs significantly from the value 1.0 ± 0.05 eV obtained earlier for the case of electronic emission from Li and means that the photoemission from Li occurs into the medium different from that for Au and SnCd.

The w value is the difference between the Fermi level of the electrons in the metal and the potential well minimum in the medium, into which the emission occurs. The values of $w(0)$ determined in the present work allow one, using a tabulated value of the work function from Li into a vacuum, to construct the energy diagram of the Li|PF|solution interface. There are literature data on the values of the Li work function of 2.28–3.10 eV; we used the recommended value of 2.38 eV [46]. The width of the band gap for lithium compounds, which are typical ionic compounds, is a rough estimation, since for LiCl $E_g = 9.5$ eV and for LiF $E_g = 11$–12 eV [46, 47]. In Fig. 12 the schematic energy diagram of the Li|Li_2O|PC interface is presented, as obtained from our photoelectrochemical measurements.

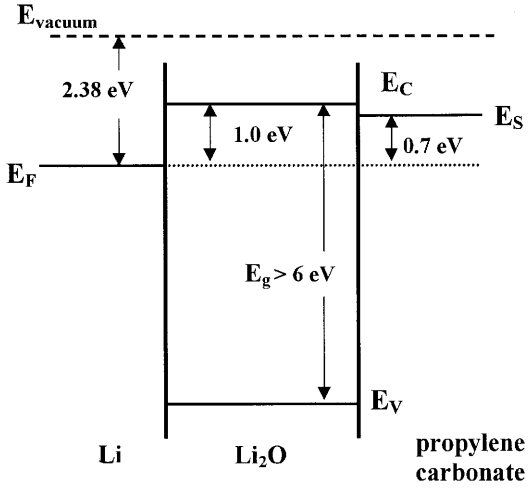

Fig. 12 Energy diagram of Li|Li_2O|PC interface. The positions of the Fermi level E_F, the level of the energy of a solvated electron in solution E_S, and the edges of both the conduction band E_C and the valence band E_V are marked

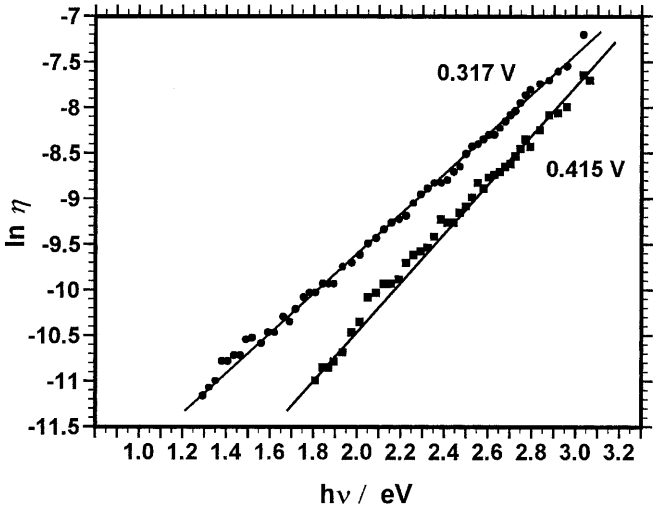

Fig. 13 Spectral dependences of the photocurrent with the Li_xSn_4Cd electrode in 1 M $LiClO_4$ in PC. Electrode potentials (relative to Li/Li^+) are indicated on the figure

Photoeffect on LiSnCd electrode

Figure 13 depicts the spectral dependences of the photocurrent obtained with the SnCd electrode after electrochemical intercalation of lithium from solution. In the course of the Li^+ ions intercalation, the silver-white electrode darkened. Since the LiSnCd electrode is reversible in the lithium salts solution, a relatively narrow range of equilibrium potentials of the alloy was used for the measurements. Consequently, it has been established with a high degree of reliability that the spectral dependences are straight lines for $\ln I_{ph}$ versus $h\nu$ (a linear correlation coefficient R^2 in different experiments assumed the values of 0.98–0.999). The coefficients of the linear regression equation, $\ln I_{ph} = a + b \times h\nu$, depend on the potential (composition of the alloy): a decreases and b somewhat increases with the gain in E (diminution of the Li concentration in the alloy).

Such spectra are not characteristic for photoemission. The exponential dependence of the photocurrent upon the absorbed light quantum energy obeys the Urbach empirical rule (Eq. 2) and presumably means, in the given case, the occurrence of an internal photoeffect in the surface layer. Thus the slope of the straight lines is $b = \gamma/kT$, from which $\gamma \approx 0.06$–0.07. For amorphous semiconductors, greater values of the γ coefficient are commonly observed, although its meaning is not clear [21, 22]. From such plots the optical width of the band gap can be also determined, since E_G^{opt} corresponds often to a short-wave beginning of an Urbach tail. For de-

termining E_G^{opt}, different methods are used; for instance, from the intersection point of a family of curves. Our data establish at least the fact that for the passivating film on LiSnCd alloy, E_G^{opt} is close to or somewhat greater than ~3 eV.

In relation to the differences in the photoelectrochemical properties of Li and LiSnCd electrodes, it would be relevant to mention the chemical properties of the PF forming on the surface of the SnCd alloy in the course of lithium intercalation into it from a $LiClO_4$ solution in PC. Information of a such kind was extracted in [39] by the method of secondary ion mass spectrometry. The surface layer of the LiSnCd electrode appeared to consist essentially of the same compounds as does a PF on Li in the PC solution, apart from that tin is also revealed [39]. We will be confined here to establishing the nature of the photoeffect with the LiSnCd electrode, the investigation of its properties as a semiconductor in detail being not within the framework of the present paper and is a subject for further study.

Conclusions

The photoelectrochemical behaviour of the Li electrode in a number of lithium salts in nonaqueous solutions used in lithium batteries has been studied. On the basis of spectral and current-voltage characteristics of the quantum yield of the photocurrent, it has been established that the photoprocess on the Li electrode is due to electronic photoemission from the metal into a solid passivating film coating a surface of the Li electrode. For this process at the equilibrium potential of the Li/Li^+ electrode, the threshold energy values for photoemission have been determined to be 1.0 ± 0.05 eV into Li_2O, 0.8 ± 0.05 eV into Li_2CO_3, and 1.3 ± 0.05 eV into LiCl. It has been confirmed that in anhydrous propylene carbonate solutions, the internal part of the passivating film consists of Li_2O, and on increasing the water content in the electrolyte the replacement of Li_2O by Li_2CO_3 occurs. The oxide film transformation into the chloride film in thionyl chloride has been revealed. In contrast to the Li electrode, for several inert electrodes (Au and SnCd) the electronic photoemission into a solution has been established within the range of the electrodes perfect polarization, that is used for determining the electronic work function into propylene carbonate, which appears to be 0.7 ± 0.05 eV at the equilibrium potential of the Li/Li^+ electrode. Li cathodic intercalation into the SnCd alloy leads to a change in the photoeffect nature: an internal photoeffect in the electrode surface layer occurs instead of photoemission. The measured values of work function have been used for constructing the energy diagram of the Li|film|electrolyte interface. Photoemission spectroscopy has been proposed for determining the chemical composition of the passivating layers on the Li electrode in lithium batteries.

Acknowledgements The authors are grateful to the Russian Foundation for Basic Research (projects 97-03-32619 and 99-03-32320) for financial support for the present work.

References

1. Gabano JP (ed) (1983) Lithium batteries. Academic Press, New York
2. Peled E (1979) J Electrochem Soc 126: 2047
3. Peled E, Golodnitsky D, Ardel G, Eshkenazy V (1995) Electrochim Acta 40: 2197
4. Yen SPS, Shen D, Vasquez RP, Grunthaner FJ, Somoano RB (1981) J Electrochem Soc 128: 1434
5. Kanamura K, Shiraishi S, Tamura H, Takehara Z (1994) J Electrochem Soc 141: 2379
6. Kanamura K, Tamura H, Shiraishi S, Takehara Z (1995) J Electrochem Soc 142: 340
7. Kanamura K, Tamura H, Takehara Z (1992) J Electroanal Chem 333: 127
8. Schwager F, Geronov Y, Muller RH (1985) J Electrochem Soc 132: 285
9. Aurbach D, Daroux ML, Faguy PW, Yeager E (1987) J Electrochem Soc 134: 1611
10. Aurbach D, Gofer Y (1991) J Electrochem Soc 138: 3529
11. Aurbach D, Ein-Ely Y, Zaban A (1994) J Electrochem Soc 141: L1
12. Osaka T, Momma T, Matsumoto Y, Uchida Y (1997) J Electrochem Soc 144: 1709
13. Naoi K, Mori M, Shinagawa Y (1996) J Electrochem Soc 143: 2517
14. Nazri G, Muller RH (1985) J Electrochem Soc 132: 2050
15. Kasahara N, Nishihama H (1987) J Power Sources 20: 265
16. Aurbach D, Zaban A, Schechter A, Ein-Eli Y, Zinigrad E, Markovsky B (1995) J Electrochem Soc 142: 2873
17. Ishikawa M, Yoshitake S, Morita M, Matsuda Y (1994) J Electrochem Soc 141: L159
18. Kovač M, Milićev S, Kovač A, Pejovnik S (1995) J Electrochem Soc 142: 1390
19. Gurevich YuYa, Pleskov YuV, Rotenberg ZA (1980) Photoelectrochemistry. Consultants Bureau, New York
20. Stimming U (1986) Electrochim Acta 31: 415
21. Mott NF, Davis EA (1979) Electron processes in noncrystalline materials, 2nd edn. Clarendon Press, Oxford
22. Lubchenko AF, Zushman JM (1969) Phys Status Solidi 32: 703
23. Brodskii AM, Gurevich YuYa, Levich VG (1970) Phys Status Solidi 40: 139
24. Fowler RH (1931) Phys Rev 38: 45
25. Pleskov YuV, Rotenberg ZA (1969) J Electroanal Chem 20: 1
26. Rotenberg ZA, Gromova NV, Kazarinov VE (1986) J Electroanal Chem 204: 281
27. Rotenberg ZA, Gromova NV (1986) Elektrokhimiya 22: 152
28. Rotenberg ZA, Nekrasova NV (1989) Elektrokhimiya 25: 114
29. Nimon ES, Churikov AV, Gamayunova IM, Lvov AL (1993) J Power Sources 43: 157
30. Nimon ES, Churikov AV, Kharkats YuI (1997) J Electroanal Chem 420: 135
31. Modestov AD, Nimon ES, Rotenberg ZA, Churikov AV (1996) Russ J Electrochem 32: 705
32. Fauteux D, Koksbang R (1993) J Appl Electrochem 23: 1
33. Anani A, Crouch-Baker S, Huggins RA (1988) J Electrochem Soc 135: 2103
34. Kanamura K, Toriyama S, Shiraishi S, Takehara Z (1995) J Electrochem Soc 142: 1383
35. Aurbach D (1989) J Electrochem Soc 136: 906
36. Aurbach D, Gottlieb H (1989) Electrochim Acta 34: 141
37. Aurbach D, Daroux M, Faguy P, Yeager E (1991) J Electroanal Chem 297: 225
38. Aurbach D, Zaban A (1995) J Electrochem Soc 142: L108
39. Nimon ES, Churikov AV (1996) Electrochim Acta 41: 1455

40. Churikov AV, Nimon ES, Lvov AL (1997) Electrochim Acta 42: 179
41. Churikov AV, Gamayunova IM, Shirokov AV (2000) J Solid State Electrochem 4: 216
42. Nimon ES, Churikov AV, Shirokov AV, Lvov AL, Chuvashkin AN (1993) J Power Sources 43: 365
43. Nimon ES, Churikov AV, Senotov AA, Lvov AL (1995) Elektrokhimiya 31: 350
44. Churikov AV, Kharkats YuI (1999) Russ J Electrochem 35: 385
45. Gamayunova IM, Churikov AV (1999) Russ J Electrochem 35: 1000
46. Grigoriev IS, Meilikhov EZ (eds) (1991) Physical quantities. Energoatomizdat, Moskow
47. West AR (1984) Solid state chemistry and its applications. Wiley, New York